

Platelets drive thrombus propagation in a hematocrit and glycoprotein VI dependent manner in an in vitro venous thrombosis model

Marcus Lehmann, Rogier M. Schoeman, Patrick J. Krohl, Alison M. Wallbank, Joseph R. Samaniuk, Martine Jandrot-Perrus, and Keith B. Neeves

Materials

Bovine serum albumin (BSA), calcium chloride, magnesium chloride, sodium chloride, hydrochloric acid, HEPES, glucose, Fluorinert FC-40, 3,3'-dihexyloxacarbocyanine iodide (DiOC₆), acetone, and ethanol were from Sigma Aldrich (St. Louis, MO, USA). Sylgard 184 Silicone Elastomer Kit was from Krayden (Westminster, CO). Innovin lipidated tissue factor (TF) was from Dade-Behring (#10445705, Miami, FL). KMPR 1050 and KMPR 1010 were from MicroChem Corporation (Westborough, MA). Human fibrinogen was from Enzyme Research Laboratory (South Bend, IN) and labeled with Alexa-555 labeling kit purchased from Life Technologies (Grand Island, NY). (Tridecafluoro-1,1,2,2-tetrahydrooctyl)trichlorosilane was from Gelest (SIT8174.0, Morrisville, PA). Annexin V binding buffer (Cat #422201) and Pacific Blue Annexin V label (Cat # 640918) were from Biolegend (San Diego, CA). Abciximab was a gift from the University of Colorado Hospital. Atopaxar was from Adooq Biosciences (Cat #A13813, Irvine, CA). Human D-dimer was from Abcam (Cat #ab98311, Cambridge, MA). ACT017, a GPVI blocking humanized Fab fragment was a gift from Anticor Biotech (Paris, France). 3 µm FITC-labeled polystyrene beads (PSF-003UM) were from Magsphere (Pasadena, CA). Cover glass and plastic syringes (60 mL, BD, Cat #309653 and 3 mL BD, Cat #309657) were purchased from Fisher Scientific (Waltham, MA, Cat # 12-544-18). Biopsy punches, 0.75 mm and 1.5 mm, were from World Precision Instruments (Sarasota, FL, Cat #504529) and Ted Pella (Redding, CA, Cat #15110-15), respectively. Small tubing (Tygon S-54-HL PVC Medical Tubing, 0.010" ID, Tygon S-54-HL PVC Medical Tubing, 0.03" ID) was from Cole Parmer (Vernon Hills, IL). Connectors (1/16" T Type, Cat# 64028) and large tubing (1/16" ID, Cat #57739) were from US plastics (Lima, Ohio). The 500 µL gastight glass syringe was from Hamilton (Reno, NV, # 81220). 10X HEPES Buffered Saline (HBS) was prepared by dissolving 1500 mM NaCl and 250 mM HEPES in deionized (18.2 MΩ-cm) water. 10X HBS was diluted to 1X using deionized water prior to use. RBC wash buffer (10 mM HEPES, 140 mM NaCl, 1 % w/w glucose, pH =7.3) was made in house. Recalcification buffer (75 mM CaCl₂, 37 mM MgCl₂ pH= 7.4 in HBS) was made in house. Normal pooled plasma (NPP) was from George King Biomedical (Overland Park, KS, Cat #0010-5).

Microfluidic device fabrication

Two consecutive layers of KMPR 1050 (MicroChem, Newton, MA) photoresist were spun at 1500 rpm on a silicon wafer, with a 20 min soft bake (100 °C) following each spin coat. The photoresists was exposed to a UV light dose of 2608 mJ/cm², followed by a 3 min hard bake (100 °C) and development in 2.38% tetramethylammonium hydroxide (AZ MIF 300). The device height was measured with profilometry to be 145 µm. Wafers were pretreated with (tridecafluoro-1,1,2,2-tetrahydrooctyl)trichlorosilane for four hours prior via vapor deposition under vacuum before each molding. PDMS was poured on the wafer at a 10:1 ratio of base to catalyst and the wafer was cured in a convection oven for 4 h at 60 °C. The mold was peeled and inlet and outlet holes (0.75 mm) and a vacuum hole (1.5 mm) were defined with biopsy punches. The PDMS device was cleaned with successive sonication in 1 M HCl, acetone, and ethanol for 5 min each followed by a

forced air dry. The device was placed in a 60 °C oven overnight to fully dry. It was then covalently bonded to cover glass via oxygen plasma (100W, 45 seconds) and then placed in a 60 °C oven overnight.

Supplemental Tables

Supplemental Table I. Flow rates as a function of hematocrit and Re for plasma as the bulk fluid.

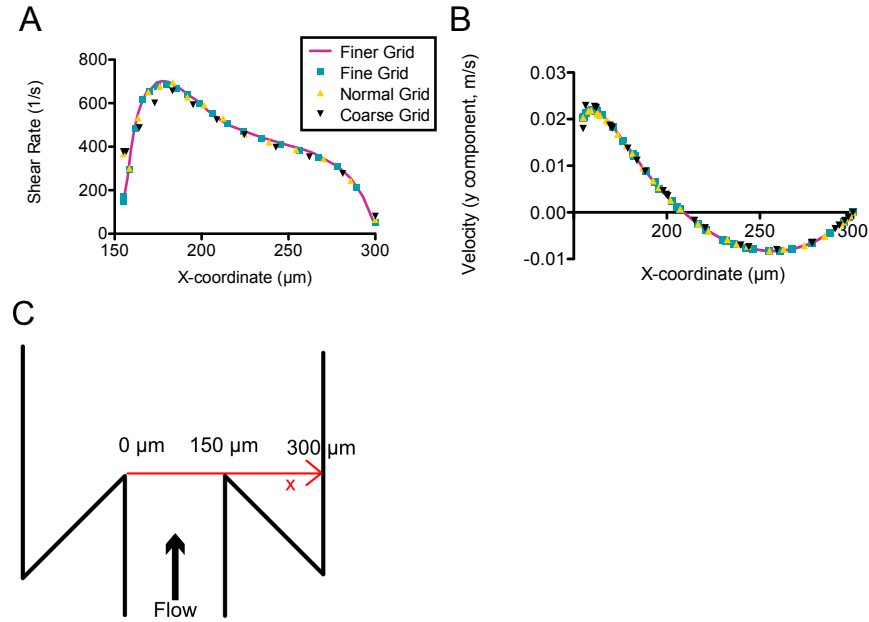
Plasma	HCT 0	HCT 0.2	HCT 0.4	HCT 0.6
Re = 0.1	1.5 $\mu\text{L}/\text{min}$	2.3 $\mu\text{L}/\text{min}$	3.7 $\mu\text{L}/\text{min}$	5.9 $\mu\text{L}/\text{min}$
Re = 1	15 $\mu\text{L}/\text{min}$	23 $\mu\text{L}/\text{min}$	37 $\mu\text{L}/\text{min}$	59 $\mu\text{L}/\text{min}$
Re = 10	148 $\mu\text{L}/\text{min}$	235 $\mu\text{L}/\text{min}$	372 $\mu\text{L}/\text{min}$	592 $\mu\text{L}/\text{min}^*$
Re = 25	370 $\mu\text{L}/\text{min}$	586 $\mu\text{L}/\text{min}$	930 $\mu\text{L}/\text{min}$	1479 $\mu\text{L}/\text{min}$

* For thrombus formation experiments the HCT 0.6 case was run at 372 $\mu\text{L}/\text{min}$ due to volume constraints.

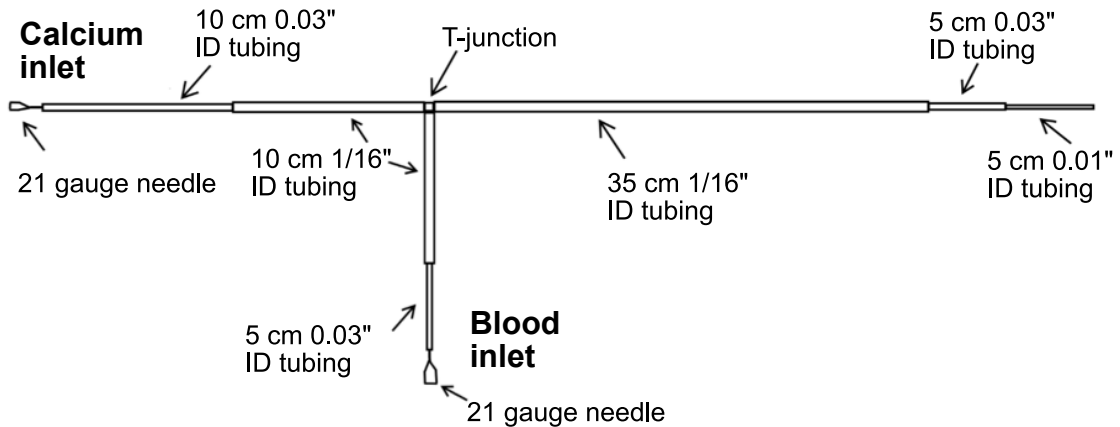
Supplemental Table II. Flow rates as a function of hematocrit and Re for buffer as the bulk fluid.

Buffer	HCT 0	HCT 0.2	HCT 0.4	HCT 0.6
Re = 0.1	0.9 $\mu\text{L}/\text{min}$	1.3 $\mu\text{L}/\text{min}$	2.0 $\mu\text{L}/\text{min}$	3.3 $\mu\text{L}/\text{min}$
Re = 1	9 $\mu\text{L}/\text{min}$	13 $\mu\text{L}/\text{min}$	20 $\mu\text{L}/\text{min}$	33 $\mu\text{L}/\text{min}$
Re = 10	90 $\mu\text{L}/\text{min}$	135 $\mu\text{L}/\text{min}$	204 $\mu\text{L}/\text{min}$	329 $\mu\text{L}/\text{min}$
Re = 25	225 $\mu\text{L}/\text{min}$	337 $\mu\text{L}/\text{min}$	509 $\mu\text{L}/\text{min}$	821.7 $\mu\text{L}/\text{min}$

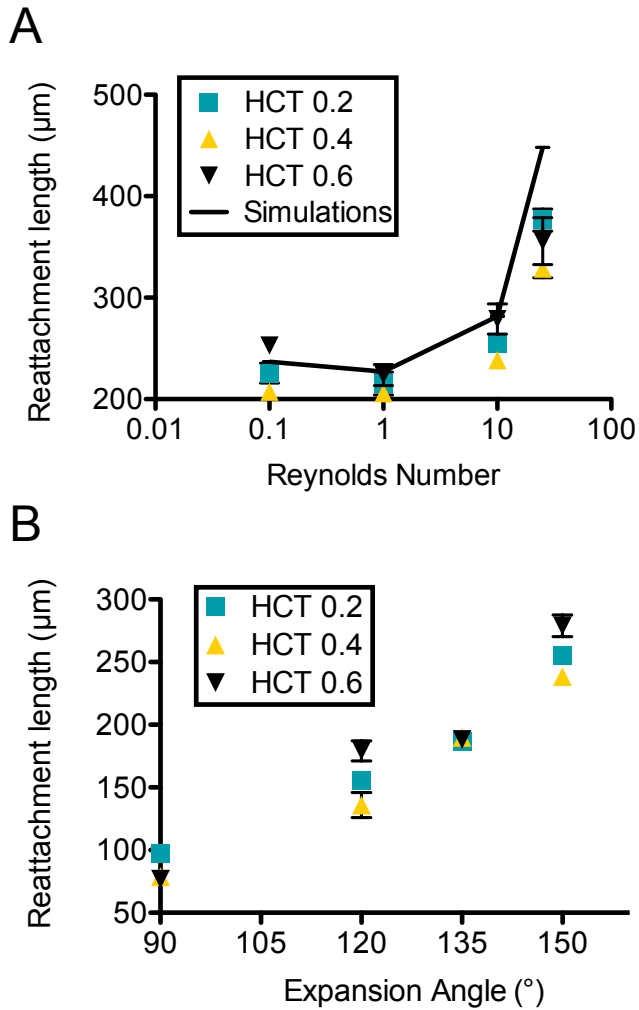
Supplemental Figures



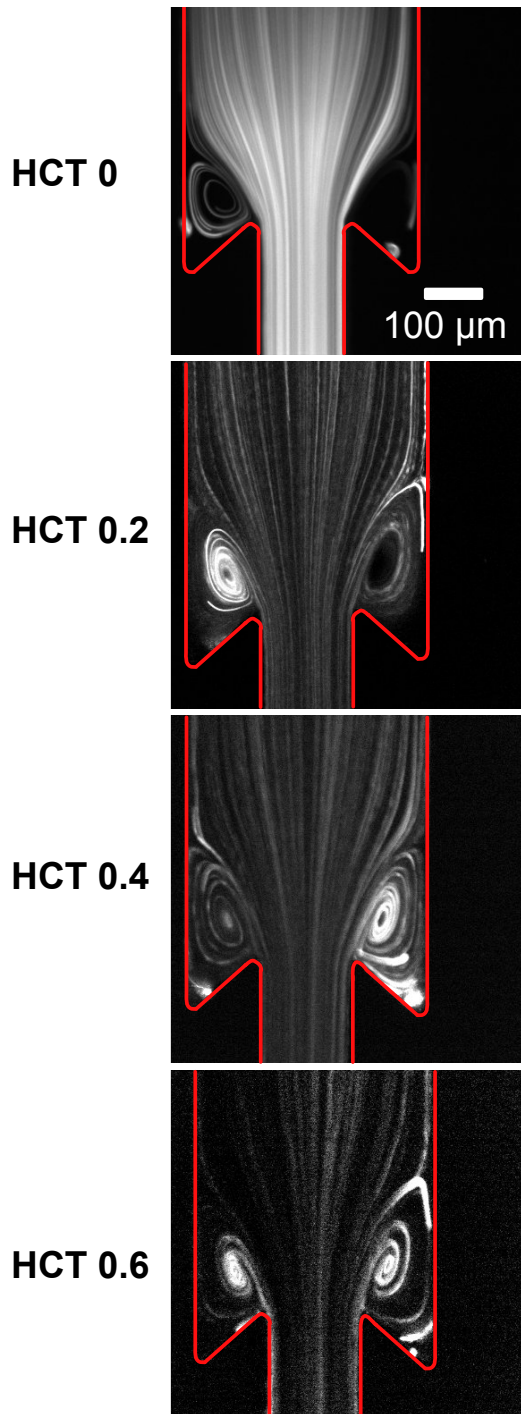
Supplemental Figure I. Wall shear rate (A) and velocity in the direction of bulk flow (B) plotted from the expansion point to the wall for the 150° expansion at $Re = 10$ for different mesh sizes. The coarse grid results deviate at the edges, but the other results show good agreement. (C) Schematic of the computational geometry including x-axis corresponding to (A) and (B). Note shear rates and velocity in (A) and (B) correspond to the line defined by the expansion point ($x = 150 \mu\text{m}$) to the wall ($x = 300 \mu\text{m}$).



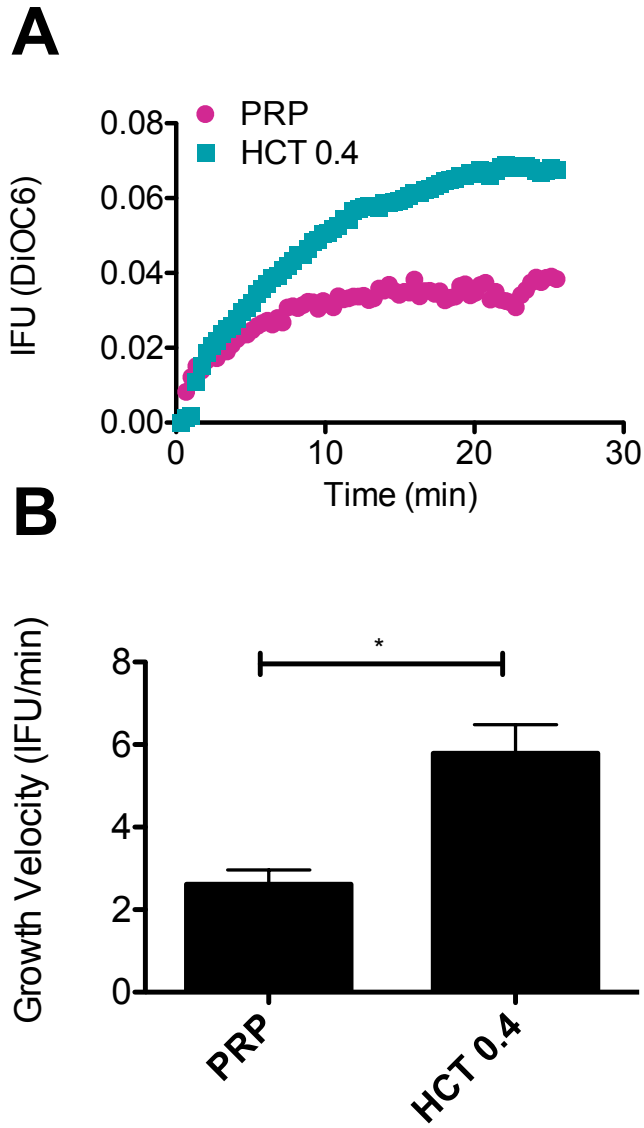
Supplemental Figure II. Tubing connection setup. Lengths and tubing diameters are listed.



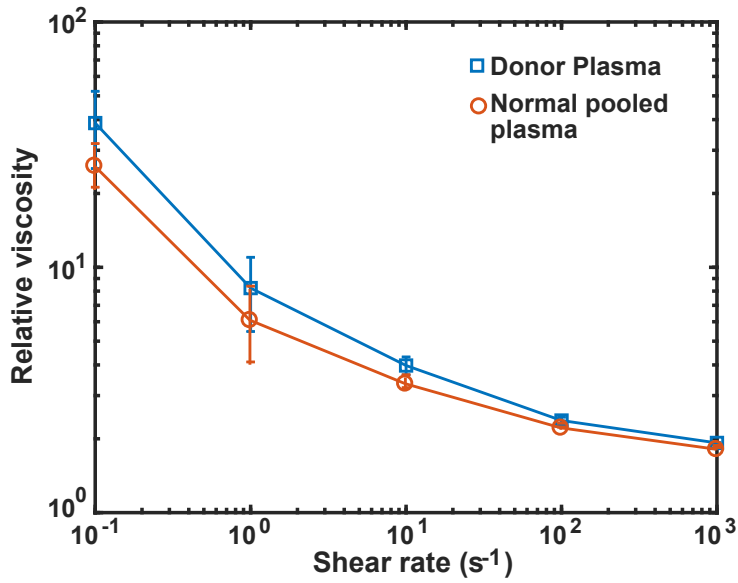
Supplemental Figure III. (A) The flow reattachment length as a function of Re measured experimentally at HCT 0.2, 0.4, and 0.6, as well as from the simulations for the 150° expansion angle. (B) The flow reattachment length at $Re = 10$ for HCT 0.2, 0.4, and 0.6 as a function of expansion angle. Error bars in both plots represent SEM ($n = 3$).



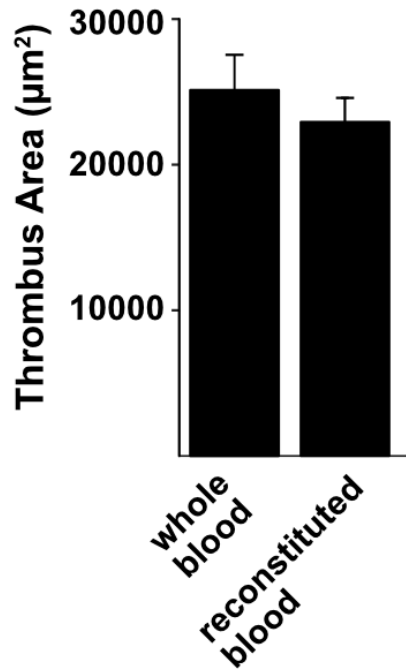
Supplemental Figure IV. Streaklines for the 135° expansion angle at $Re = 25$ for HCT of 0, 0.2, 0.4 and 0.6.



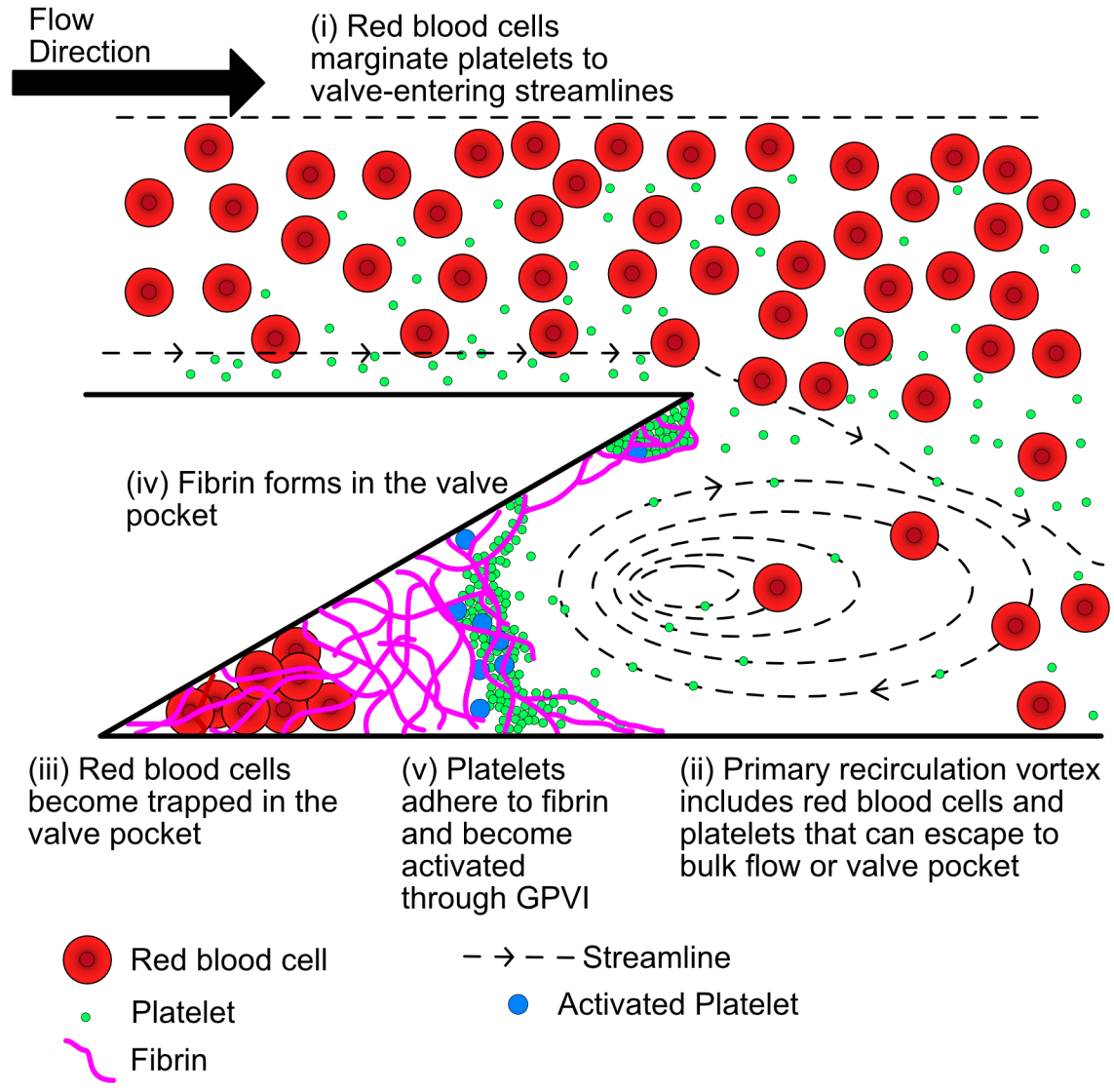
Supplemental Figure V. Platelet accumulation in the valve pocket is increased in the presence of RBC. (A) Characteristic plots of cumulative platelet accumulation in the valve pocket as measured by integrated fluorescence intensity (IFU) if DiOC₆ labeled platelets for platelet rich plasma (PRP) and reconstituted blood at HCT 0.4, both at $Re = 10$. (B) Mean growth velocity of the platelet accumulation for PRP and reconstituted blood. Error bars represent SEM, $p = 0.0213$ (Mann-Whitney U-test).



Supplemental Figure VI. Relative viscosity of RBC suspended in autologous donor plasma or normal pooled plasma at a HCT = 0.4. The relative viscosity is the measured suspension viscosity divided by the measured plasma viscosity (no RBC). Each data point represents the average and standard deviation of $n = 6$ measurements. There was no significant difference (Mann-Whitney U-test) in viscosity at any shear rate between the two suspensions.



Supplemental Figure VII. Thrombus area at 30 minutes for whole blood from (n = 6 donors, HCT = 0.38-0.51) and reconstituted blood (n = 6 donors, HCT = 0.4) perfused at $Re = 10$ through TF-coated devices. The means and standard errors are plotted. There was no statistical difference as measured by the Mann-Whitney U-test.



Supplemental Figure VIII. Proposed mechanism of the propagation of the thrombus in the in vitro model. RBC-mediated margined platelets enter the primary recirculation vortex under hemodynamic conditions that result in flow separation. Fibrin can form in the low shear region of the valve pocket with or without cells. Platelets in the presence of RBC can adhere to and aggregate at the fibrin interface and become activated through GPVI, and for a subpopulation of platelets PS positive. These PS positive platelets provide additional coagulation sites and help propagate the thrombus into the vessel lumen.

Supplemental Video Legends

Supplemental Video 1: Particle streakline timelapse for HCT 0, 0.2 and 0.4 at Re of 1, 10, and 25 for the 150° expansion. Exposure time is 100 ms. Time between frames 1 s.

Supplemental Video 2: Brightfield overview of the thrombus formation at Re = 10, of reconstituted blood (HCT 0.4) through the 150° expansion. RBC are entrapped in the first minutes. The formation of platelet rich and RBC rich regions is visible at 12 minutes.

Supplemental Video 3: Confocal images of the thrombus formation at Re = 10 through the 90° expansion for PRP and reconstituted blood. DiOC₆ is in green and labeled fibrin(ogen) is in red.

Supplemental Video 4: Confocal images of the thrombus formation at Re = 10 through the 150° expansion for PNP, PRP, PNP with RBC (HCT 0.4) and reconstituted blood (PRP, HCT 0.4). DiOC₆ is in green and labeled fibrin(ogen) is in red. The DiOC₆ is absorbed by the PDMS walls, which highlights the geometry even in the absence of platelet adhesion.

Supplemental Video 5: Control confocal images of the thrombus formation at Re = 10 through the 150° expansion for PNP, PRP, PNP with RBC (HCT 0.4) and reconstituted blood (PRP, HCT 0.4) without TF on the surface. DiOC₆ is in green and labeled fibrin(ogen) is in red.